Mechanical behavior of entangled fibers and entangled cross-linked fibers during compression

Laurent Mezeix · Christophe Bouvet · Julitte Huez · Dominique Poquillon

Abstract Entangled fibrous materials have been manufactured from different fibers: metallic fibers, glass fibers, and carbon fibers. Specimens have been produced with and without cross-links between fibers. Cross-links have been achieved using epoxy spraying. The scope of this article is to analyze the mechanical behavior of these materials and to compare it with available models. The first part of this article deals with entangled fibrous materials without cross-link between fibers. Compression tests are detailed and test reproducibility is checked. In the second part, compression tests were performed on materials manufactured with cross-linked fibers. The specific mechanical behavior obtained is discussed.

Introduction

Entangled materials are made from natural materials (wool, cotton, etc.) as well as artificial ones (steel wool, glass wool, etc.). Bonded metal fiber network materials offer advantages [1–7] for use, like heat exchanger [8] or insulation [9]. Indeed, they present a low relative density, high porosity, and simplicity of production by cost-effective routes with considerable versatility concerning metal composition and network architecture. On the other hand, sandwich panel consists of two thin skins separated by a thick core. Core material is usually in the form of honeycomb, foam, or balsa. Recently, a novel type of sandwich has been developed with bonded metallic fibers as core material [10–15]. This material presents an attractive combination of properties like high specific stiffness, good damping capacity, and energy absorption. Metal fibers are bonded with a polymeric adhesive [15] or fabricated in a mat-like form and consolidated by solid state sintering [12]. Entangled cross-linked carbon fibers have been also studied for use as core material by Laurent Mezeix [16]. Indeed entangled cross-linked carbon fibers present many advantages for application as core material: open porosity, multifunctional material, or possibility to reeve electric or control cables on core material. Only a few studies have so far been devoted to the mechanical behavior of fiber compression. However, some data are available regarding wood fibers [17, 18], glass fibers [19], and various matted fibers [20]. But few studies are devoted to the mechanical behavior of material made from entangled cross-linked fibers [21].

Models to understand the mechanical behavior of fibrous material have been proposed by van-Wyk [22], Toll [23], and Castéra [18]. van-Wyk considered a random distribution of fiber orientations. Only the bending behavior of fibers is modeled and the macroscopic law in compression is:

$$\sigma = a\exp(b\varepsilon) \tag{1}$$

where a and b are negative constants, σ is the stress and ε the strain. The exponent b is a function of the fibers organization: $b = -3$ for a 3D random structure [20] and $b = -5$ for 2D random plane structure [22]. Castéra [18] proposes a phenomenological macroscopic law of compression for wood fibers. Modeling using finite elemental methods [24] and molecular dynamics simulations [25, 26]

L. Mezeix (✉) · J. Huez · D. Poquillon
Université de Toulouse, CIRIMAT, INPT-ENSIACET, 118 route de Narbonne, 31077 Toulouse, France
e-mail: laurent.mezeix@ensiacet.fr

L. Mezeix · C. Bouvet
Université de Toulouse, UPS, LGMT, Bat 3PN 118 route de Narbonne, 31062 Toulouse Cedex, France

are also available. But, due to the number of fibers and number of contacts between fibers, these simulations take into account a small number of fibers and/or fibers with a small aspect ratio (<200).

In the present article, fibers have been chosen in function of their nature, application, and cost. Due to their high performance, carbon fibers are intensely used in many applications: aeronautics, sport equipments, or high performance vehicles. Glass fibers are widely used, because of their low cost, in many applications like thermal insulation for pipe, building. Bonded metal fiber network are used as core material [10–15]. The purpose of the present study is to analyze and to model the mechanical behavior of materials made from these three types of fibers with and without cross-link. So, two families of materials have been studied: entangled fibers and entangled cross-linked fibers. In the first part, the mechanical behavior of entangled fibers has been investigated and the experimental curves have been compared with the available model. In the second part of the article, cross-linked fibrous materials have been described and their mechanical properties during compression tests have been investigated and analyzed.

Materials and methods

Material elaboration

Carbon fibers (12 K) consist of a yarn of stranded carbon filaments. Fibers were provided by Toho Tenax. The Young modulus of the carbon fiber is 240 GPa. Fibers diameter is 7 μm and the initial epoxy coating represents 1 wt%. Assuming that the coating is uniform, then its thickness is about 30 nm. Stainless steel fibers were provided by UGITECH. Fibers diameter is 12 μm and the Young modulus is 180 GPa. Glass fibers are obtained from yarns that were provided by the company PPG Fiber glass. Fibers diameter is 12 μm and their Young modulus is about 73 GPa. Figure 1 shows the cut fibers.

For aeronautical applications, many sandwich-panel skins are made using carbon/epoxy prepreg. That is the reason why epoxy resin has been chosen for cross-linking fibers. Epoxy resin was provided by the company SICOMIN. The provided resin has a low viscosity (285 mPa s) and polymerization duration is 2 h at 80 °C.

For all the tests carried out during this work, specimens are carefully weighted using SARTORIUS balance (±10 μg). Resin is heated up to 35 °C to decrease viscosity and thus allow a better vaporization. A paint spray gun (Fiac UK air compressors) is used to spray epoxy. Materials were observed using a Scanning Electron Microscope (LEO435 VP) operating at 15 kV.

For all the materials manufactured in the present study, the fiber length equals 40 mm. Two different architectures have been tested: entangled fibers and entangled cross-linked fibers. Table 1 summarizes different fiber architectures tested. As the relative density of the material need to be as low as possible, a previous study has shown that the yarns size needs to be decreased by separating the filaments [27]. In the previous work, epoxy coating of carbon yarns was removed by the following chemical treatment. The carbon fibers were treated in a solution of dichloromethane for 24 h, and then cleaned for a lapse of time of 2 h in methanol [28]. Then, the uncoated carbon fibers were hand carded to achieve the entanglement. In this study, separation of carbon yarns was obtained owing to a blower room. The air fluxes of this blower room are sufficient for separating carbon fibers of the 40 mm long yarn without removing the initial epoxy coating. So a comparison will be made between materials manufactured from separated entangled carbon fibers, with or without this initial coating (see Table 1). The blower room was also used for glass fibers and steel fibers separation (to decrease yarn size).

Table 1 Fiber architectures tested

Fibers	Architecture	
	Entangled fibers	Entangled then cross-linked fibers
Stainless steel fibers	Separated	Separated and cross-linked
Carbon fibers	Yarns (12 K)	Separated and cross-linked
	Separated yarns	
	Separated and uncoated yarns	
Glass fibers	Separated	Separated and cross-linked

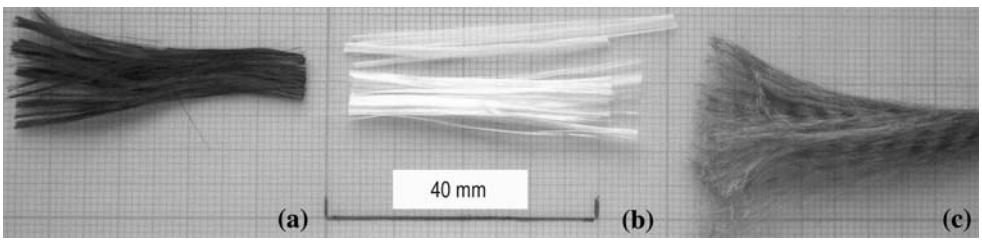

Fig. 1 Initial fibers after been cut (40 mm): **a** carbon yarn, **b** glass fibers, and **c** stainless steel fibers

For all the materials manufactured in the present study, entanglement is obtained using a controlled air flow in the specific blower room. Then the entangled fibers can be taken out, and tested (entangled architecture) or they can be cross-linked before the process (entangled then cross-linked architecture). In that case, epoxy is sprayed using paint spray gun during the final minutes of the entanglement.

As for core application, one key parameter is the density. We have chosen to perform tests on entangled fiber materials with different fiber densities (100, 150, and 200 kg/m^3). As the volume of the mold is known and the fibers mass is carefully weighted and the volumetric density is controlled. For cross-linked architectures, only one density is tested (150 kg/m^3). It is important to notice as the density of bulk carbon in the carbon fibers (1760 kg/m^3) is lower than the glass fibers one (2530 kg/m^3), which is lower than stainless steel (7860 kg/m^3), the relative volumetric density of the tests materials differs. Table 2 summarizes the data of the different materials tested.

Many SEM observations have been taken so remarks made on pictures present in this study can be generalized. Figure 2 shows a typical SEM observation on carbon fibers. We can notice the high number of cross-links between fibers on Fig. 2a. Figure 2b shows a high resolution image of a typical cross-link between two carbon fibers. Figure 3 shows a typical SEM observation on cross-linked stainless steel fibers. We can notice clearly that the entanglement is better on stainless steel fibers than on separated carbon fibers. The effect of Young modulus is less noticeable due to the plasticity and remaining strain at the epoxy joints. We can also observe that the roughness of stainless steel fibers is more important than the one made of carbon fibers. However, if the architecture made from stainless steel presents a higher entanglement, a smaller proportion of epoxy cross-links is achieved compare to the carbon fibers material manufactured in the same condition or to the material made from glass fibers (Fig. 4). Number of epoxy cross-link are an average obtained by many SEM observations.

Table 2 Relative volumetric density for different materials tested (Architecture without cross-link)

	Density of the entanglements (kg/m^3)	Fiber volume fraction
Stainless steel fibers	100	0.013
Ø = 12 μm	150	0.019
E = 180 GPa	200	0.025
Carbon fibers	100	0.057
Ø = 7 μm	150	0.085
E = 240 GPa	200	0.114
Glass fibers	100	0.040
Ø = 12 μm	150	0.059
E = 80 GPa	200	0.079

Compression tests

The quasi-static compressive response of entangled fibers was measured in a screw-driven test machine MTS with a 5 kN load cell. For material made of entangled fibers (not cross-linked), samples are introduced between the lower and the upper part of the specific device (Fig. 5a). Sample diameter is 60 mm. Initial sample height is for all types of fiber and for all densities tested equal to 30 mm. Initial stress is applied to maintain the initial height. So these compression tests are carried out in die (confined compression tests).

For the materials made with cross-linked fibers, the sample is introduced between the punches and the compression test is then carried out (no lateral confinement). The sample size in this case is 30 × 30 × 30 mm^3 (Fig. 5b). In both case, the punch velocity is $v_0 = 1.8$ mm min^{-1} corresponding to a nominal strain rate of $\dot{\varepsilon} = 10^{-3}$ s^{-1}.

To analyze the experimental results, we used the usual following definition for the true strain and true stress:

$$\varepsilon = \ln\left(\frac{h}{h_0}\right) \tag{2}$$

$$\sigma = \frac{F}{S}$$

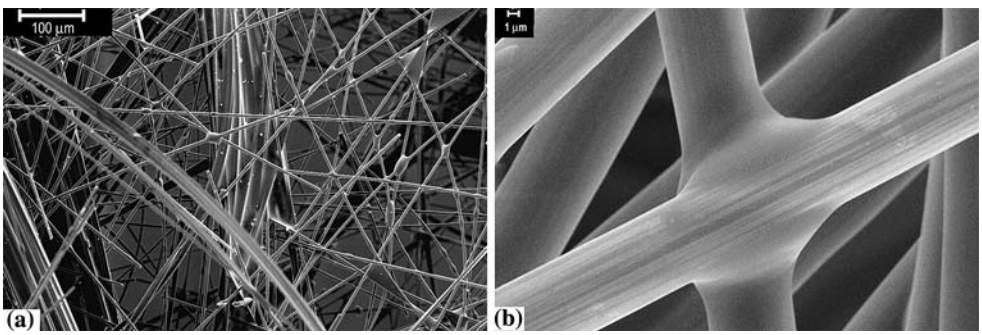

Fig. 2 SEM observation **a** separated then cross-linked carbon, and **b** zoom on a typical cross-linked between two carbon fibers

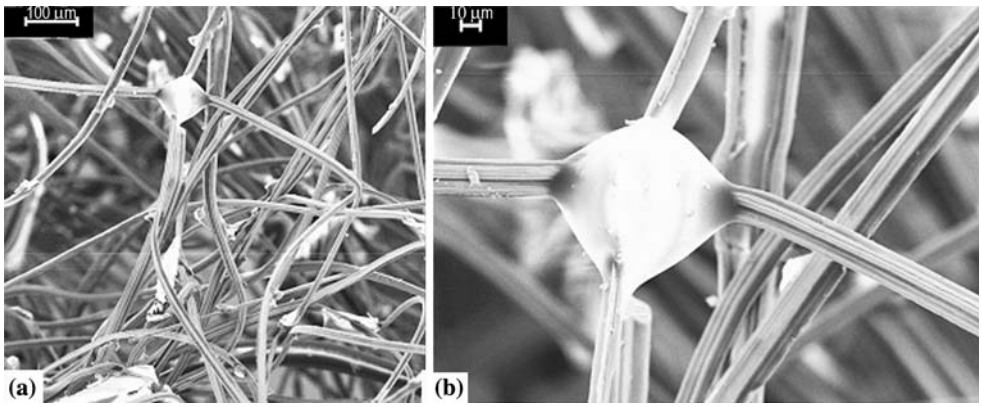

Fig. 3 SEM observation **a** cross-linked stainless steel fibers, and **b** zoom on a typical cross-linked between two stainless steel fibers

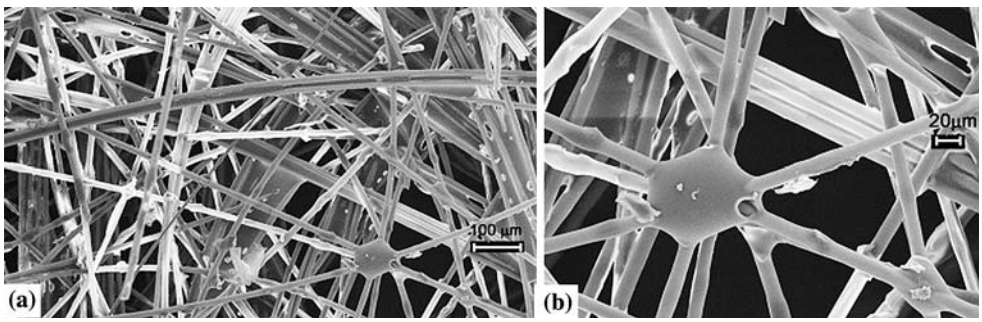

Fig. 4 SEM observation **a** cross-linked glass fibers, and **b** zoom on a typical cross-linked between glass fibers

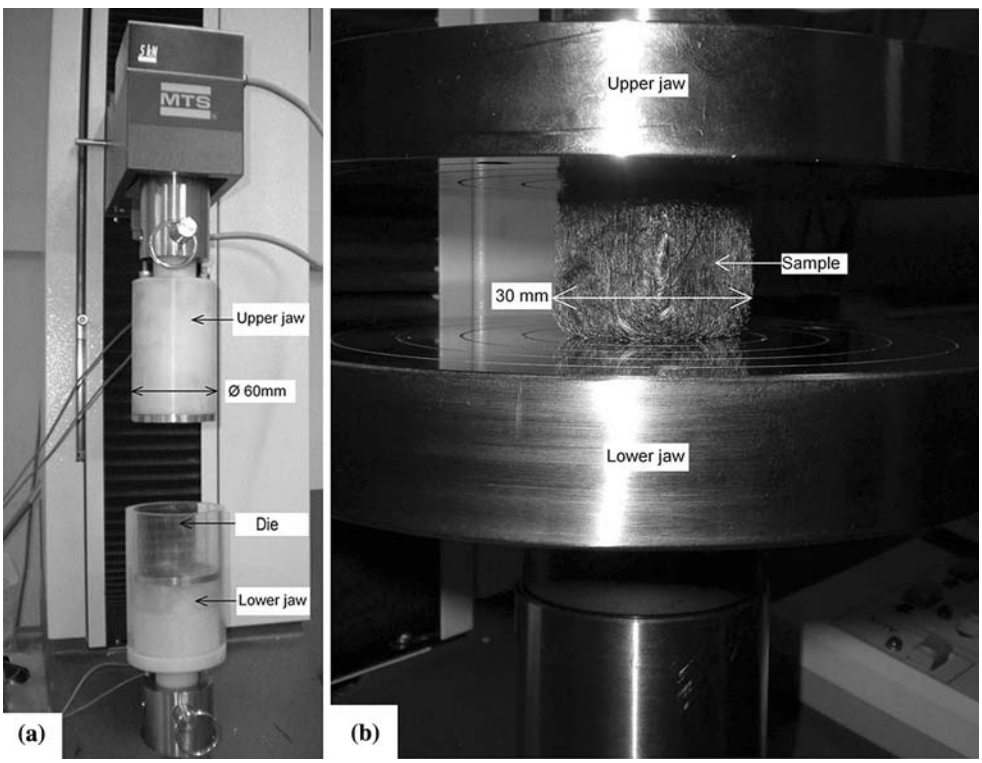

Fig. 5 **a** Specific device for compression on entangled fibers, and **b** devise for cross-linked fibers

where h is sample length, h_0 the initial sample length, and F the applied load on the section S of the specimen. For entangled then cross-linked architecture, S_0 equals 900 mm^2 and for entangled materials S_0 equals 2827 mm^2. In the first case $S_0 = S$ due to the confinement. In the second case in the stress range tested, there is no significant modification of the surface area and $S_0 \approx S$.

Results and discussion

Materials made with entangled fibers

Entangled carbon fibers

As listed in Table 1, three different architectures of porous material are made using carbon fibers: entangled yarns which have the largest fiber section (12 K), separated and entangled yarns with coated or uncoated fibers.

Figure 6 shows results from compression tests on each of these architectures for a 150 kg/m^3 material (fiber volume fraction is then 8%). Three compression tests were done in each case to check the reproducibility of test. We can notice that the shape of the curve is comparable for all the architectures. This is due to the rearrangement of the fibers during the compression. We can also notice that the reproducibility is very good for uncoated and separated fibers. This point may be due to the quality of the entanglement and due to its isotropy which is easier to achieve with the separated fibers than with the yarns. Furthermore, epoxy coating seems not to have an effect on the mechanical behavior in compression. The results are similar to those obtained for separated and uncoated fibers. In fact, as the thickness of this epoxy coating is less than 1% of the thickness of the fiber, a minor effect on the stiffness of the fiber was expected. However, surface modification could indicate wear conditions, fibers motion, and rearrangement. Experiment evidences only a minor effect during compactions. So, the presence of the epoxy nano-scale at the surface of the fiber does not change significantly the sliding and the motion of fibers during compression.

A slight discrepancy is observed during compression tests for materials made of carbon yarns. This is due to the yarn size. The material manufactured with yarns is less isotropic because more yarns are parallel to the bottom of the compression device (Fig. 5a). So the regularity and the isotropy of the architecture are pretty more difficult to obtain. The largest strain under the same compression stress is obtained with this material, which is likely due to the yarns alignment during the compression (perpendicular to the load axis). Separated yarns with coated or uncoated fibers are stiffer due to a better entanglement. More fibers remain in the direction of the main stress and for a given stress a smaller strain level is reached. For materials made with carbon fiber, for a given density, the less the fiber diameter size is the higher the stiffness is. With smaller fiber diameter the quality of the architecture is better. So the number of 'beam' contacts obtained is increased and the length between contacts decreased. The mechanical behavior during compression test is similar between separated yarns and separated and uncoated yarns. Removing the initial epoxy coating is not necessary and from now on, this step will be skipped.

Effect of the fiber nature

For materials made with the same initial density (150 kg/m^3), Fig. 7 compare results of compression tests for glass fibers and stainless steel fibers. We can notice the good reproducibility of compression tests carried out on these two types of entangled fibers. Figure 8 show curves obtained for separated carbon fibers, carbon yarns, stainless steel, and glass fibers. For the same initial density (i.e.,

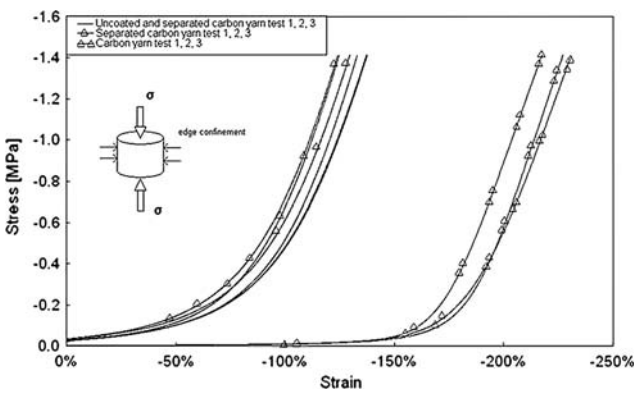

Fig. 6 Stress/strain curves of different architectures obtained from materials with an initial density of 150 kg/m^3 made with entangled carbon fibers

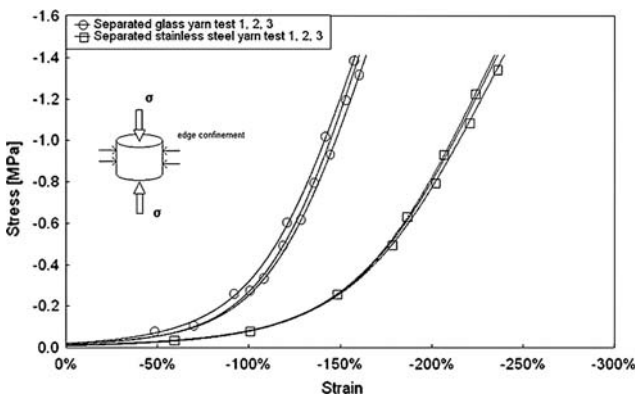

Fig. 7 Stress/strain curves of different architectures obtained from material with an initial density of 150 kg/m^3 made glass fibers and stainless steel fibers

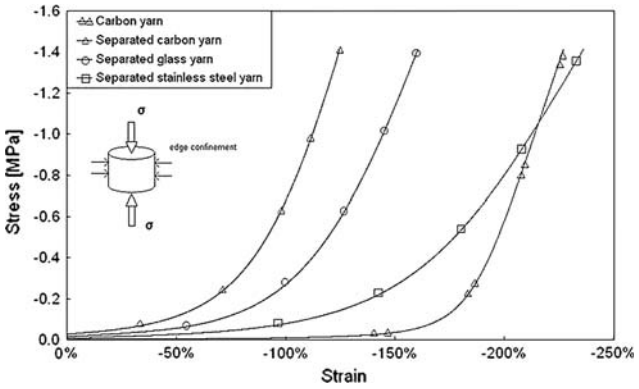

Fig. 8 Comparison of 150 kg/m^3 materials behavior in compression for different fibers natures

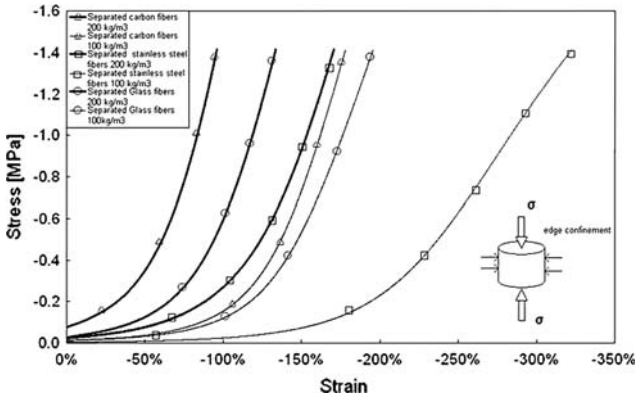

Fig. 9 Comparison of compression stress/strain curves for different initial densities

150 kg/m^3), the relative volumetric density of the material made with carbon fibers is larger than the relative volumetric density of the material made with glass fiber (Table 2). So the distance between contacts in the entanglement is smaller on carbon fibers. Even if the carbon fibers diameter is smaller than that of the glass fibers, the Young modulus of the carbon fibers is 3 times the one of the glass fibers. So the rigidity of the microscopic beam between contacts is larger for carbon fibers and the macroscopic strain smaller. Densification of the material made with stainless steel fibers appear after densification of the one made of separated carbon fibers. But, due to plasticity at the contact between fibers, strain localization induced large bending for the stainless steel fibers and the macroscopic deformation is larger for a given stress.

To obtain the highest stiffness for an application as core material, the material made with separated carbon fibers is the better choice. But due to the higher cost of carbon fibers compared to glass fibers, this material could be a good choice.

Effect of the initial density of material

Effect of density has been studied on separated carbon fibers, stainless steel, and glass fibers. Densities used are 100, 150, and 200 kg/m^3. Figure 9 shows effect of the density for 100 and 200 kg/m^3 on compression. Initial stress is due to the initial conditions (see "Compression tests" section). The higher the density, the higher is the initial stress needed to have a height of 30 mm. For each material, as the initial density increases, compression curves move from the right to the left and densification starts for smaller strain. For separated stainless steel fibers the densification slop of sample with density of 100 kg/m^3 is lower than the other density.

Parkhouse and Kelly [29] provide the maximum packing concentration of 3D long straight fibers distributed randomly in space. The volume fraction is given by:

$$Vf = 2\frac{\ln\left(\frac{L}{D}\right)}{L/D} \tag{3}$$

where L is the length of fibers (40 mm) and D the diameter. For carbon fibers Eq. 3 gives a value of 0.003 and for the glass and stainless steel fibers it gives 0.004. Fiber volume fractions of the samples tested in this study are given in Table 2. The maximum packing concentration given by Eq. 3 is lower than these values but the fibers used in this study are not straight, so packing concentration obtained is larger than the one given by Eq. 3.

Modeling

Eleven tests have been carried out on entangled materials. The compression curves are fitted using Eq. 1. Figure 10 shows the van-Wyk model fit realized on entangled carbon fibers with a density of 150 kg/m^3. We have also tried to fit the experimental data with the Castéra model [18] but the results obtained were not in so good agreement. So, in the following part, we will focus only on the van-Wyk model that fits well the whole curve for all the tests carried out. Table 3 details coefficients obtained by fitting the curves and the confidence interval of the model. The value of r^2, the square of correlation coefficient is also given indicating that the fit are quit good except for carbon yarn. The exponent b is between -1.6 and -3.95. van-Wyk exponent for carbon yarns is the highest (in absolute value) compared to the other samples. This point confirms that the entanglement achieved with carbon yarns is less isotropic. Indeed modelings detailed in [22] and in [23] show that the value of this exponent for isotropic entanglement is -3 whereas it is -5 for 2D isotropic material (isotropy in the plane perpendicular to the load). The Toll coefficient of separated carbon fibers is pretty closed from -3, so the material made by separated carbon fibers is isotropic. For the different materials tested, the van-Wyk exponent

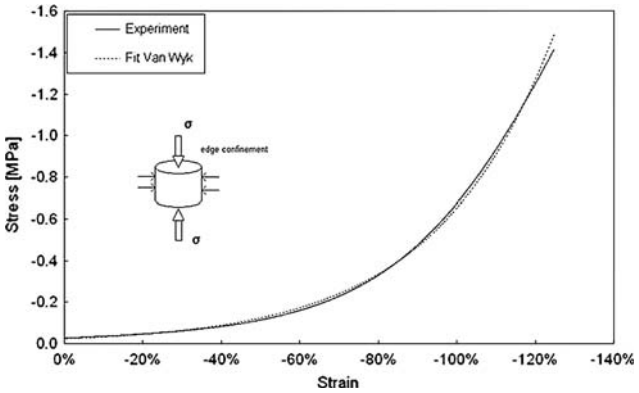

Fig. 10 Compression stress/strain curve for entangled separated carbon fibers, initial density = 150 kg/m^3, fit following Eq. 1

increases when initial density of the material increases. Higher is the density, near is the exponent from the value −3. It means the isotropy is better when the density increases. In the case of separated carbon yarn, the isotropy is already obtained for the density of 150 kg/m^3. For separated glass and stainless steel yarn with the density of 200 kg/m^3 the isotropy is not obtained yet. We can also observe that there is no significant difference between the exponent of uncoated and separated carbon fibers, and exponent are about −3. Although for glass fibers, exponent is just under 3 (in absolute value). The lowest values are for stainless steel fibers. But, in that case, SEM observations show that the fibers are not at all linear. A large entanglement is observed due to local plastification of the stainless steel fibers. So the model of bending beam developed in [23] is no longer suitable.

In order to improve the stiffness of the materials manufactured in the first part of this study without increasing their density [27] cross-links were realized by spraying epoxy resin owing to a paint spray gun in order to block the contact between fibers. Results of compression tests on improved architecture are now detailed.

Materials made with cross-linked fibers

Cross-linked fibers samples have been tested in compression. Density used for each type of fibers is 150 kg/m^3. The initial fiber density of the material is determined as explained above. After that, resin is sprayed into the sample, which is weighted again after epoxy polymerization. So the additional mass of resin can be measured and the added quantity is about 50 kg/m^3.

Figure 11 shows a comparison of the compression behavior of separated entangled carbon fibers with or without epoxy cross-link. As expected, the cross-linking increases the initial stiffness of the material. For a given strain level, the stress level for strain under 80 % is strongly increased. Initial stress for entangled carbon fibers is due to the initial test condition (see "Compression tests" section). For higher strain, densification occurs and the curves are comparable. This behavior means that the cross-links are progressively broken which is confirmed by post-mortem SEM observations. Furthermore, tests are quite reproducible.

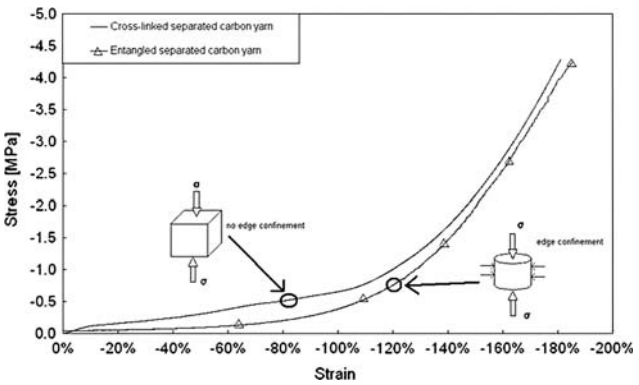

Fig. 11 Compression stress/strain curves of materials made with separated carbon fibers, with or without cross-linked, initial density = 150 kg/m^3

Table 3 Fit of the curves obtained during compression test of materials made with entangled fibers without epoxy cross-link

Material	Fibers density (kg/m^3)	Model of van-Wyk–Toll (Eq. 1)		
		a	b	r^2
Carbon yarn	150	$-0.00018 \times 10^6 \pm 0.0003$	-3.94 ± 0.21	0.965
Separated carbon fibers	100	-0.0103×10^6	−2.81	0.997
	150	$-0.028 \times 10^6 \pm 0.005$	-3.17 ± 0.16	0.999
	200	-0.0761×10^6	−3.07	0.999
Uncoated carbon fibers	150	$-0.021 \times 10^6 \pm 0.001$	-3.09 ± 0.09	0.999
Stainless steel fibers	100	-0.0109×10^6	−1.60	0.983
	150	$-0.013 \times 10^6 \pm 0.0007$	-2.01 ± 0.04	0.995
	200	-0.025×10^6	−2.39	0.999
Glass fibers	100	-0.011×10^6	−2.50	0.995
	150	$-0.019 \times 10^6 \pm 0.003$	-2.74 ± 0.08	0.997
	200	-0.032×10^6	−2.87	0.998

Confidences intervals are obtained by reproducibility tests on sample with 150 kg/m^3 density. The tests for the other density are not duplicated. r^2 is the square of correlation coefficient

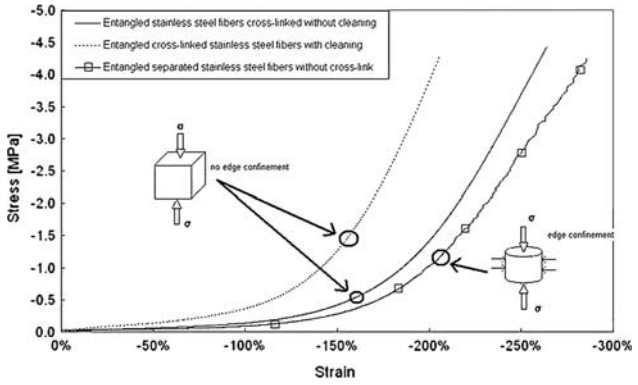

Fig. 12 Compression stress/strain curves of materials made with separated stainless steel fibers, with or without cross-linked, initial density = 150 kg/m^3

Results obtained for stainless steel fibers are detailed in Fig. 12. The first point to notice is that without cleaning fibers, the materials obtained after epoxy cross-linking offers poor improvement. SEM observations (Fig. 3) confirmed that the number of cross-links is inferior to what is observed for material made with carbon fibers. To increase stiffness due to the cross-links, stainless steel fibers need to be degreased. Fibers are cleaned 10′ in ethanol followed by a second cleaning of 10′ in acetone. Stainless steel fibers with degreasing present a better bonding which is evidenced on Fig. 12. However, as expected, the stiffness of this material is bellow the one obtain with carbon fibers (Fig. 14).

The last architecture to test was the one obtained by cross-linking the entangled glass fibers. The result of compression test is illustrated on Fig. 13. Clearly, the stiffness of the material is really increased. We can notice a large effect on the initial stiffness. When densification occurs, cross-links are progressively broken. SEM observations of samples tested less than 4.3 MPa in compression show that a large proportion of cross-links remains.

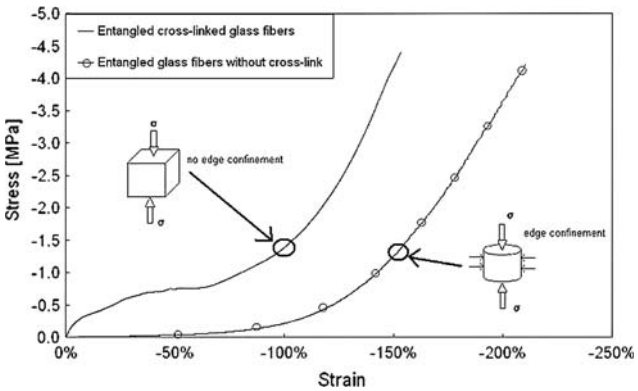

Fig. 13 Compression stress/strain curves of materials made with separated glass fibers, with or without cross-linked, initial density = 150 kg/m^3

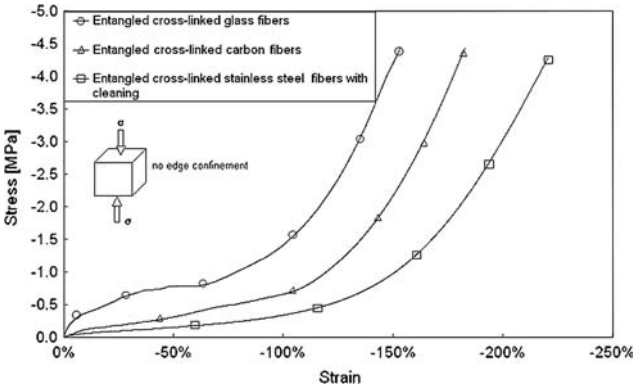

Fig. 14 Comparison of compression stress/strain curves of architectures made with separated fibers, with cross-linked, initial density = 150 kg/m^3

Figure 14 shows comparison between materials made with cross-linked carbon fibers, stainless steel fibers, and glass fibers. Contrary to the behavior of the material without cross-link, the better stiffness is achieved with the glass fibers. Furthermore, the plateau level [30] of stress during compression is quite high. Densification is the dominant mechanism for strain above 70%. Table 4 gives the values of the initial stiffness of the materials obtained and the average stress level of the plateau before densification. The initial stiffness of the cross-linked glass fibers is 8.4 MPa. For glass fibers and carbon fibers, the second part of the compression curves, which corresponds to the behavior observed in the first part of this study (without cross-link) was fitted with the van-Wyk–Toll model. The exponent is, respectively, −2.07 for glass fibers and −2.36 for carbon fibers. These values are to be compared with those obtained on sample without cross-link and with a fiber density of 150 kg/m^3 (Table 3). We can notice that with epoxy cross-link exponent values decrease. The presence of the epoxy bonding changes the boundary conditions of the bending beams and fibers are not free to slip. Furthermore, epoxy spraying effect may also have changed slightly the isotropy of the entanglement. Compression tests on transverse direction might be done to clarify this hypothesis.

In order to get a better understanding of the macroscopic behavior of the cross-linked architecture, important microscopic information is the average distance d_{av} between two cross-links. An analysis of SEM pictures has been carried out and results are given in Table 5. As expected after the comparison on the compression behavior, the shortest distance d_{av} is obtained for glass fibers. This is the reason why the initial stiffness of the material is better when compared to the deflection of the beam which depends on the cubic of the distance between two cross-links. This point was not expected as the relative density of the entanglement is higher for the carbon than for the glass. Different surface

Table 4 Cross-linked architecture manufactured in this study initial density, initial stiffness, and average stress during the compression plateau

Material	Fibers density (kg/m^3)	E (MPa)	σ plateau (MPa)
Separated and cross-linked stainless steel fibers	150	0.6	0.25
Separated and cross-linked carbon yarn	150	1.1	0.4
Separated and cross-linked glass yarn	150	8.4	0.8

Table 5 Comparison of distances between cross-links

Material	Number of contacts per fiber, $\langle c \rangle$	Average distance, d_{av}, between joints calculated using Eq. 4 (mm)	Average distance, d_{av}, between joints observed by SEM measurements (mm)
Separated and cross-linked stainless steel fibers	127	0.31	0.30
Separated and cross-linked carbon yarn	974	0.04	0.20
Separated and cross-linked glass yarn	395	0.10	0.15

properties, different reactivity with the epoxy could explain that point.

There are many discussions about the determination of the average distance between fiber contacts. Authors have proposed models to quantify the number of contacts per fiber, in layered structures [31, 32], and in 3D network fibers [23, 33, 34]. The average number of contacts per fiber $\langle c \rangle$, in the case of 3D random network, is given by:

$$\langle c \rangle = 2\frac{L}{D}f \tag{4}$$

where L is the length of fibers (40 mm), f the volume fraction of fibers, and D is the diameter. Knowing the length of fibers and the average number of contacts per fiber obtained by the Eq. 4, the distance, d_{av}, between joints can be obtained by $d_{av} = L/\langle c \rangle$. Results for d_{av} calculated are given in Table 5. Importantly, density used is the same for all fibers (150 kg/m^3) but the volumetric concentration is not the same (Table 2). We can notice that the distance between joints obtained by Eq. 4 is closed from SEM observations for glass and stainless steel fibers. In the case of carbon fibers, the difference is important. Further investigations on the microscopic organization of the material manufactured in that study are still necessary. X-ray tomography measurement would provide more valuable information.

Clyne et al. developed a simple analytical model based on the bending of inclined individual fiber segments [21, 35, 36], the Young's modulus is given by:

$$E_a = \frac{9E_f f}{32\left(\frac{d_{av}}{D}\right)^2} \tag{5}$$

where E_f is the Young's modulus of fibers, f the volume fraction of fibers, d_{av} is the length between joints, and D the fiber diameters. The value obtained with this approach may be compared with the one given by Gibson and Ashby for the similar type of material [30]. This is also based on beam deflections, but with a more constrained geometry. Assuming simply supported cylindrical beams lying parallel or normal to the applied load. The Young's modulus predicted is expressed as follows:

$$E_a = \frac{3\pi E_f}{4\left(\frac{d_{av}}{D}\right)^4} \tag{6}$$

Using the experimental data obtained for the initial stiffness of the material (Table 4) and knowing the fibers diameters, Young modulus has been calculated applying Eqs. 5 and 6 and are given in Table 6. We can notice that the Young modulus obtained by Eq. 6 is closed to the experimental values for carbon and glass fibers. This point could mean that the epoxy drop at the cross-link limits the

Table 6 Comparison of Young modulus

Material	E: Young modulus (MPa)		
	Calculated using Eq. 5	Calculated using Eq. 6	E_{exp}
Separated and cross-linked stainless steel fibers	1.7	1.2	0.6
Separated and cross-linked carbon yarn	7.3	0.8	1.1
Separated and cross-linked glass yarn	7.8	7	8.4

deflection of fibers. In the case of stainless steel fibers, the difference between experiment and Eq. 6 could be explained by the plastification of fibers.

Tomography data before the compression test and at the beginning of the plateau would be very useful to determine the fibers orientation, the isotropy of the initial entanglement, the average number of contacts per fiber, and could help to get a better understanding of the fiber slippage and fiber orientation changes induced by compression. This last point is underlined by Zhu et al. [37] and has never been studied before.

Conclusion

Original materials have been manufactured using entangled fibers. Three different families of fibers have been tested: glass fibers, carbon fibers, and stainless steel fibers. Different architectures and different initial densities were used during compression tests. For entangled fibers without cross-link, the best stiffness was obtained for separated carbon fibers. The compressing behavior of the isotropic material fabricated follows the van-Wyk model. In order to improve this stiffness and contacts between fibers have been bonded using epoxy cross-links. The material obtained remains light (200 kg/m^3) as the process developed in this study optimizes the quantity of epoxy used. The best stiffness is obtained for glass fibers mainly because the shortest distance between cross-links is compared to the carbon case. The initial stiffness of the cross-links architecture seems to follow the model proposed by Ashby.

Acknowledgements Financial support for this work was obtained thanks to a BQR (Bonus Qualité Recherche) of the University of Toulouse and thanks to funding provided by the region Midi-Pyrénées (CEFICAS project).

References

1. Ducheyne P, Aernoudt E, Meester P (1978) J Mater Sci 13(12):2650. doi:10.1007/BF00552695
2. Clyne TW, Mason JF (1987) Metal Trans A 18(8):1519
3. Delannay F, Clyne TW (1999) In: Proceedings of the 1st international conference on metal foams and porous metal structures (MetFoam'99), Bremen, Germany, 14–16 Jun 1999
4. Yamada Y, Wen CE, Chino Y, Shimojima K, Hosokawa H, Mabuchi M (2003) Mater Sci Forum 419:1013
5. Markaki AE, Gergely V, Cockburn A, Clyne TW (2003) Comput Sci Technol 63(16):2345
6. Woesz A, Stampfl J, Fratzl P (2004) Adv Eng Mater 6(3):134
7. Delince M, Delannay F (2004) Acta Mater 52(4):1013
8. Golosnoy LO, Cockburn A, Clyne TW (2008) Adv Eng Mater 10(3):210
9. Zhang BM, Zhao SY, He XD (2008) J Quant Spectrosc Radiat Transf 109(7):1309
10. Gustavsson R (1998) Patent WO 98/01295, 15th Jan 1998, AB Volvo
11. Markaki AE, Clyne TW (2001) US patent 10/000117, Cambridge University
12. Markaki AE, Clyne TW (2003) Acta Mater 51(5):1341
13. Markaki AE, Clyne TW (2003) Acta Mater 51(5):1351
14. Dean J et al (2008) In: Ferreira (ed) Proceedings of the 8th international conference on sandwich structure (ICCS8), Portugal, p 199
15. Zhou D, Stronge WJ (2005) Int J Mech Sci 47(4–5):775
16. Mezeix L, Bouvet C, Castanié B, Poquillon D (2008) In: Ferreira (ed) Proceedings of the 8th international conference on sandwich structure (ICCS8), Portugal, p 798
17. Castéra P (2002) In: Proceedings of matériaux 2002, ISBN 2-914279-08-6
18. Haeffelin JM, Bos F, Castéra P (2002) In: Proceedings of matériaux 2002, ISBN 2-914279-08-6
19. Baudequin M (2002) PhD Thesis, Université Pierre et Marie Curie Paris VI
20. Poquillon D, Viguier B, Andrieu E (2005) J Mater Sci 40(22):5963. doi:10.1007/s10853-005-5070-1
21. Clyne TW, Markaki AE, Tan JC (2005) Compos Sci Technol 65(15–16):2492
22. van-Wyk CM (1946) J Text Inst 37:285
23. Toll S (1998) Polym Eng Sci 38:1337
24. Durville D (2005) J Mater Sci 40(22):5941. doi:10.1007/s10853-005-5061-2
25. Barbier C, Dendievel R, Rodney D (2008) Numerical study of 3-D compressions of entangled materials. Comput Mater Sci. doi:10.1016/j.commatsci.2008.06.003
26. Barbier C, Dendievel R, Rodney D (2008) PhD Thesis, Institut National Polytechnique de Grenoble
27. Mezeix L (2007) Material Science Master's degree, Université de Toulouse
28. Margueritat-Regenet C (2002) PhD Thesis, Ecole National Supérieure des Mines de Paris
29. Parkhouse JG, Kelly A (1995) Proc R Soc A 451:737
30. Gibson LJ, Ashby MF (1997) Cellular solids: structure and properties. Cambridge University Press, Cambridge
31. Batchelor WJ, He J, Sampson WW (2006) J Mater Sci 41(24):8377. doi:10.1007/s10853-006-0889-7
32. He J, Batchelor WJ, Johnston RE (2007) J Mater Sci 42(2):522. doi:10.1007/s10853-006-1146-9
33. Dodson CTJ (1996) Tappi J 79(9):211
34. Phillipse AP (1996) Langmuir 12(5):1127
35. Markaki AE, Clyne TW (2004) Biomaterials 25(19):4805
36. Markaki AE, Clyne TW (2005) Acta Mater 53(3):877
37. Zhu et al (1995) Chem Eng Sci 50(22):3557